



HAL
open science

Powered Two-Wheeled Vehicles Steering Behavior Study: Vision-Based Approach

Pierre-Marie Damon, Hicham Hadj-Abdelkader, Hichem Arioui, Kamal
Youcef-Toumi

► **To cite this version:**

Pierre-Marie Damon, Hicham Hadj-Abdelkader, Hichem Arioui, Kamal Youcef-Toumi. Powered Two-Wheeled Vehicles Steering Behavior Study: Vision-Based Approach. 15 th International Conference on Control, Automation, Robotics and Vision (ICARCV 2018), Nov 2018, Singapore, Singapore. pp.355–360, 10.1109/ICARCV.2018.8581298 . hal-01933667

HAL Id: hal-01933667

<https://hal.science/hal-01933667v1>

Submitted on 4 Oct 2019

HAL is a multi-disciplinary open access archive for the deposit and dissemination of scientific research documents, whether they are published or not. The documents may come from teaching and research institutions in France or abroad, or from public or private research centers.

L'archive ouverte pluridisciplinaire **HAL**, est destinée au dépôt et à la diffusion de documents scientifiques de niveau recherche, publiés ou non, émanant des établissements d'enseignement et de recherche français ou étrangers, des laboratoires publics ou privés.

Powered Two-Wheeled Vehicles Steering Behavior Study: Vision-Based Approach

Pierre-Marie Damon^{1,2}, Hicham Hadj-Abdelkader¹, Hichem Arioui¹ and Kamal Youcef-Toumi²

Abstract—This paper presents a vision-based approach to prevent dangerous steering situations when riding a motorcycle in turns. The proposed algorithm is capable of detecting under, neutral or over-steering behavior using only a conventional camera and an inertial measurement unit. The inverse perspective mapping technique is used to reconstruct a bird-eye-view of the road image. Then, filters are applied to keep only the road markers which are, afterwards, approximated with the well-known clothoid model. This allows the prediction of the road geometry such as the curvature ahead of the motorcycle. Finally, from the predicted road curvature, the measurements of the Euler angles and the vehicle speed, the proposed algorithm is able to characterize the steering behavior. To that end, we propose to estimate the steering ratio and we introduce new pertinent indicators such as the vehicle relative position dynamics to the road. The method is validated using the advanced simulator BikeSim during a steady turn.

I. INTRODUCTION

Car manufacturers are very excited! The Powered Four-Wheeled Vehicles (P4WV) market is again on the rise, boosted primarily by the interest that portend future buyers to new technologies and autonomous vehicles. Indeed, users are gradually attracted by systems, providing optimum safety (active safety belt, shared driving or automated, Brake Assist, GPS, etc.).

For last two decades, research and development companies and researchers are very active on new ways of assisting drivers. Many of these Advanced Driver Assistance Systems (ADAS) are already unavoidable (Adaptive Cruise Control (ACC), Lane Keeping System (LKS), etc.) even mandatory (Anti-lock Braking System (ABS), Electronic Stability Program (ESP), etc.). All automotive fields are covered, more less well: traffic management and modeling, vehicle automation, study of the driver's behavior, infrastructure development, inter-vehicular communication, etc.

Unfortunately, this keen interest is not as obvious to some other road users, although they are most affected in road accidents. Indeed, according to the recent MAIDS (Motorcycle Accident In Depth Study), Powered Two-Wheeled Vehicles (P2WV) present a risk 20 times greater than that others mean of transport. In question, we can mention excessive speed, poorly adapted infrastructure, rider training level, etc. When cornering, all these risk factors lead riders to imminent danger even irremediable hazard. In France, 54% of accidents occur during a bend, without a third party involved [1]. To answer this issue, many advanced rider assistance systems

(ARAS) have been proposed. One can cite: Advanced Safety Vehicle (ASV) from Yamaha, Intelligent Speed Adaptation system (ISA) [2], and in the SAFERIDER European framework an Intelligent Curve Warning system [3].

Our present work tackles the question of the motorcycle's steering behaviour. This is achieved with vision-based techniques, by far, achievable without the need for complex computational algorithm or costly perception systems.

This paper is organized as follows. Section 2 presents the motivations and defines the problem. All the vision aspects such that the inverse perspective mapping technique, the road marker filtering and the fitting step are addressed in section 3. At the end of the same section, we present pertinent indicators to characterize the steering behavior. Whereas in section 4, simulations carried out with the advanced motorcycle simulator "BikeSim" are discussed. Finally, concluding remarks are summarized in section 5.

II. MOTIVATION AND PROBLEM STATEMENT

During a bend, riding a motorcycle requires four key-points: rider's position on the motorcycle, adjusting speed and gear ratio, direction gaze and finally motorcycle position on the road (preferable or neutral zone). Here, we are particularly interested in the last point and the detection of over or under-steering situations. Over-steering is a drift of the rear wheel greater than the front one. The bike wants to turn more than what is required or lean too much to get into the bend. As to under-steer is a drift of the front wheel more than wheel behind. The bike seems to continue straight while we steered the wheels (out of the curve situation).

Usually, it is possible to correct an under-steer by briefly releasing the throttle and slightly straightening the front wheels by counter-steering in order to recover more adhesion. This phenomenon is very often related to an excessive speed when entering in turn or an excessive acceleration at the exit. In 30% of cases, motorcyclists do not have enough time to reply to these dangerous situations [4].

From the control point of view, the over-steer is less dangerous and occurs more generally under bad weather conditions (snow, rain or icy road). The adjustment of the brake distribution may be a catch-up solution to this skid situation (similar to controlled drift for cars).

Within this context, the SAFERIDER project [5] gives a full prospection of the researches that were interested in performance and maneuverability indices during steady-state turning. These last express the correlation between neutral maneuvers and under or over-steering situations (ratio of roll angle to steering torque or ratio of speed or road curvature

¹ Authors are with University Paris-Saclay, IBISC Laboratory, Evry, France.

² Authors are with Massachusetts Institute of Technology, MRL, Cambridge, USA. pdamon@mit.edu

to steering dynamics). The most complete research is from Cossalters team [6]. The main objective is to determine the best cornering layouts and to identify a neutral driving zone. This is achieved with the quantification of the steering ratio ξ described by an explicit mathematical model. This parameter is calculated based on prior knowledge or measure of various dynamic states and geometrical features.

The major drawback of this work is the impossibility of estimating without having access to several dynamic states such as: linear and angular velocities, road curvature, roll and steer angles as well as side slip ones. Not to mention the prior knowledge of several geometric parameters of the bike (caster angle, wheelbase, etc.). It is obvious that access accurately to these data and measures, even noisy, is a very difficult challenge.

Based on our approach developed in [7], the present work attempts, beyond all the parameters mentioned above, to measure steering ratio and proposes a new vision-based approach as well as complementary steering indicators.

III. STEERING CHARACTERIZATION: ALGORITHM DESIGN

A. Vision Aspects

Camera sensor is generalized for various kinds of automotive applications. When the camera looks the road, the Bird-Eye-View (BEV) can be reconstructed using the Inverse Perspective Mapping (IPM). Indeed, the IPM creates a virtual camera removing the perspective effect. Furthermore, the IPM creates a top-view of the road making the markers easily identifiable and the obstacle detection easier. Nevertheless, the algorithms proposed for P4WV can not be extended to P2WV since the roll motion which is required when it is not considered for P4WV.

Consider a calibrated conventional camera attached to the frame \mathcal{F}_c . Let P be a 3D point of coordinates $\mathbf{P} = (X \ Y \ Z)^\top$ in the camera frame. The 3D point P is viewed by the camera into the 2D point p of homogeneous coordinates $\mathbf{p} = (u \ v \ 1)^\top$ in the image plane. For perspective conventional camera, the projection equation is given by:

$$\mathbf{p} \propto \mathbf{K} \mathbf{P} \quad (1)$$

where \propto denotes the equality up to scale and \mathbf{K} is the camera calibration matrix. Its expression is given in [7]. Note that for the sake of simplicity, the camera distortions are not considered in this study.

The IPM warps each image point p from initial image I into a new point p' of homogeneous coordinates $\mathbf{p}' = (u' \ v' \ 1)^\top$ in the BEV image I' . Since this transformation is applied to a planar object, the wrapping function is the collineation matrix denoted \mathbf{G} . The latter ensures the IPM transformation from I to I' such that:

$$\mathbf{p}' \propto \mathbf{G} \mathbf{p} \quad (2)$$

The collineation matrix \mathbf{G} can be expressed in terms of the intrinsic parameters and the Euclidean homography matrix $\mathbf{H} \in \mathbb{S}\mathbb{L}(3)$ related to a planar viewed object. Note that

\mathbf{H} depends on the rotational and translational displacement between the real camera pose providing the image I and the virtual one where I' is generated.

Let \mathcal{F}_v be the virtual camera frame attached to the P2WV. Its origin is the projection of the origin of the real camera frame \mathcal{F}_c on the road plane as illustrated in Figure 1. The virtual camera frame \mathcal{F}_v is oriented such that the X -axis is parallel to the vehicle longitudinal axis and the Z -axis points upward (perpendicular to the road). Under this assumption, all the points belonging to the road lie on the same plane XY of \mathcal{F}_v . In this case, the aim of the IPM is to generate a top-view of this plane by projecting back all the points from the captured 2D image I to the plane XY of the 3D frame \mathcal{F}_v . Finally, the BEV is obtained by cropping the top-view of the plane according to the desired Region Of Interest (ROI).

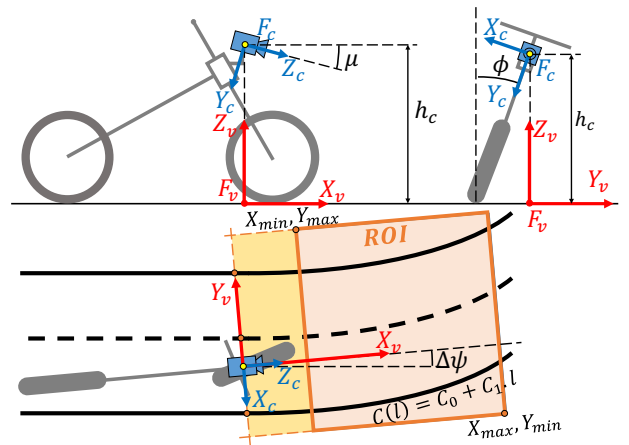


Fig. 1: P2WV & Road geometry

Under the assumptions given above, the IPM transformation based on the collineation matrix \mathbf{G} depends only on the roll and pitch angles respectively denoted ϕ and μ , the camera height h_c (see Figure 1) and the camera calibration matrices \mathbf{K} and \mathbf{K}_v (calibration matrix of the virtual camera). The latter depends on the desired resolution of the output BEV image and the ROI.

The collineation matrix \mathbf{G} can be easily identified as:

$$\mathbf{G} \propto \mathbf{K}_v \mathbf{M}^{-1} \mathbf{K}^{-1} \quad (3)$$

where

$$\mathbf{M} = \begin{bmatrix} -s_\phi s_\mu & -c_\phi & -h_c s_\phi c_\mu \\ c_\phi s_\mu & -s_\phi & h_c c_\phi c_\mu \\ c_\mu & 0 & -h_c s_\mu \end{bmatrix}$$

with s_\diamond and c_\diamond denoting respectively $\sin(\diamond)$ and $\cos(\diamond)$.

Finally, the BEV image I' is obtained by warping each point from I' onto I using the inverse mapping \mathbf{G}^{-1} . Then the image intensity is computed by interpolating the local pixels intensities in the origin image I . An example of images I and I' is given by Figure 2.

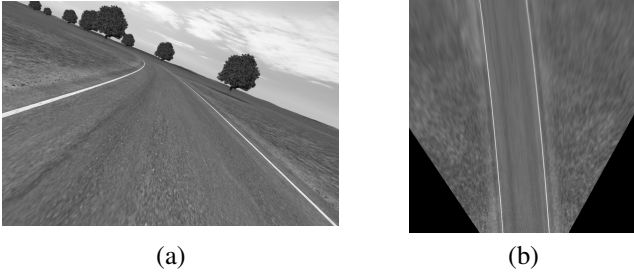


Fig. 2: Road images : (a) original image I , (b) BEV I'

B. Road Lane detection and fitting

In the race for new ADAS, the road marker detection has been widely addressed in the past years. In this work, we used the method recently proposed in [7]. It is based on the intensity gradient between the road lane markers and their surroundings. It allows the detection of both straight and curved road lanes and requires few computing resources. Moreover, this method turns out to be a very appropriate solution to detect the road lanes in a BEV image since it takes into account the line width, denoted w , as a filtering parameter. Note that the properties (width, length, etc.) are precisely defined in the road design specifications. Then the filtered image is thresholded and re-filtered to respectively keep only the lane objects in a new binary image and remove the small blobs. Once the binary image of the road lane markers I'' is obtained, one aims to separate the lanes (left, center and right in our case). To that end, a sliding window algorithm is used to track each lane independently in I'' .

When investigating the road design literature, it appears that the well-known clothoid model was largely adopted to design roads [8]. The clothoid-based design ensures smooth transitions between straight and curved lines, helping drivers to track the road markers and avoiding abrupt changes in the steering direction. It is defined such that the length of the curve l from the curve origin must be proportional to the curvature. Hence, the following expression was introduced in the literature by [9]:

$$C(l) = C_0 + C_1 l \quad (4)$$

where C_0 and C_1 are respectively the initial curvature and its rate along the curve as illustrated below in Figure 1. Note that $C_0 = 0$ and $C_1 = 0$ correspond to a straight line, $C_0 \neq 0$ and $C_1 = 0$ to a circular curve and $C_0 \neq 0$ and $C_1 \neq 0$ to a clothoid. This model is only valid for horizontal curves when the road is planar. As in [10], if we consider the heading angle between the road tangent and the vehicle X -axis is small (less than 10°), equation (4) can be approximated in the Cartesian coordinate system with:

$$y(x) \approx \Delta Y + \tan(\Delta\psi)x + \frac{1}{2}C_0x^2 + \frac{1}{6}C_1x^3 \quad (5)$$

with ΔY the lateral offset, $\Delta\psi$ the vehicle relative heading angle to the road trajectory. Note that in our case, we have chosen the right lane as the reference.

C. Steering Behavior Characterization

This subsection deals with the estimation of pertinent indicators in order to characterize the P2WV steering behavior. The first objective is to propose an alternative to the kinematic-based approach in order to estimate the steering ratio ξ . This last is well-known as an indicator of under, neutral and over-steering. A second aim is to introduce complementary conditions for steering behavior characterization. Note that, the proposed vision-based technique does not require any knowledge of the vehicle parameters, any prior estimation step or any steering encoder like for the kinematic approach.

From kinematic point of view, the steering ratio ξ is defined as the ratio between the cornering radius for ideal conditions R_0 (i.e. without tire side slips) and the actual cornering radius denoted R :

$$\xi = \frac{R_0}{R} \quad (6)$$

The latter can be found in [6] where the authors proposed to define the ideal cornering radius R_0 as follows:

$$R_0 = \frac{l}{\tan(\Delta)} = \frac{\cos(\phi)\cos(\delta) - \sin(\phi)\sin(\delta)\sin(\epsilon)}{\sin(\delta)\cos(\epsilon)} l \quad (7)$$

where Δ denotes the kinematic steering angle. For more details about its expression, the reader can refer to [11]. Finally, R_0 can be directly computed from the motorcycle parameters such that the caster angle ϵ , the wheel base l and from the measures of the roll and the steering angles respectively denoted ϕ and δ .

Still, according to [6], the actual kinematic radius R can be expressed as follows:

$$R = \frac{l}{\tan(\Delta - \alpha_f)\cos(\alpha_r) + \sin(\alpha_r)} = \frac{v_x}{\dot{\psi}} \quad (8)$$

where α_f and α_r denote the front and rear side slip angles. While the terms v_x and $\dot{\psi}$ correspond respectively to the longitudinal speed and the yaw rate. Regarding (8), there are two possibilities to compute the actual radius R . The first one is to equip the P2WV with an Inertial Measurement Unit (IMU) and a speedometer providing the measures of v_x and $\dot{\psi}$. The second solution, more complex, is to use a prior estimation step to estimate the side slip angles α_f and α_r . Indeed, these last are unmeasurable and their estimation is still an open topic with recent publications as in [12]. Nevertheless, most of the time these algorithms are tricky and require additional sensors.

Remark 1: Finally, once the steering ratio ξ is computed, it directly reflects the vehicle steering behavior such that:

- $\xi < 1$: Under-steering
- $\xi = 1$: Neutral steering
- $\xi > 1$: Over-steering

In addition, $\xi < 0$ corresponds to the counter-steering, which is a specific phenomena of P2WV when entering in a curve and $\xi = \infty$ means the steering behavior is critical.

For more information about the kinematic-based approach the reader can refer to [11], [6], where the authors proposed a complete investigation.

Our innovating technique is based on the use of vision. Indeed, the kinematic approach requires the exact knowledge of some P2WV parameters in (8) and a prior estimation step or the use of an encoder which is tricky to install. From practical point of view, the space around the steering column is quite small to integrate an encoder and it is hard to properly align the sensor and the steering rotation axis. In addition, the small steering angle amplitude, generally included between -5 and 5 degrees, involves the use of an accurate sensor. Our approach overcomes this problem and can be easily installed on any motorcycle without any restriction. We propose to estimate the steering ratio thanks to computer-vision.

Let us consider that the motorcycle is equipped with a front module including a camera and an IMU. Since in most of the countries, speedometers are mandatory for road vehicles, we will consider that the measurement of the longitudinal speed v_x is available. Let us remind that the vision-based algorithm introduced in the previous section allows to predict the road geometry parameters such that the road curvature and its rate. They are respectively denoted C_0 and C_1 . In addition, it estimates the relative heading angle $\Delta\psi$ and the lateral position ΔY between the P2WV to the road markers. As for the kinematic technique, we proposed to estimate the steering ratio ξ which is a key index for steering behavior characterization. To that end, the actual steering ratio R given in equation (8) can be directly computed using the measurements. Nevertheless, our contribution is about the estimation of the ideal radius R_0 . Since $R_0 = 1/C_0$, the vision-based prediction of the road geometry allows to directly estimate this variable.

Moreover, we propose to introduce the time derivatives of $\Delta\psi$ and ΔY which turn out to be great steering indicators as well. Although, ΔY is the P2WV relative lateral distance to the considered road marker (see (5)), its time derivative $\dot{\Delta Y}$ is absolute and the constant term is removed. Consequently, the time derivation of ΔY facilitates the characterization of the steering behavior. Indeed, it amplifies the signal variation from zero leading to the following findings:

- $\dot{\Delta Y} < 0$: under-steering
- $\dot{\Delta Y} = 0$: neutral steering
- $\dot{\Delta Y} > 0$: over-steering

Note that the observation can be done for $\Delta\psi$. Nevertheless, the simulations show that its dynamics is much more noisy, which make this variable a background steering indicator.

IV. BIKESIM SIMULATION RESULTS

This section validates the proposed approach during a steady turn using the advanced motorcycle simulator BikeSim which is the motorcycle version of CarSim. Let us remind that the objectives are to figure out pertinent

indicators for over and under-steering detection. To that end, the steering ratio is estimated using vision and other indicators are proposed to strengthen the detection.

The camera has been virtually installed in front of the P2WV at a height $z_c = 1.10$ m and mechanically tilted of an angle $\mu_0 = 15^\circ$. Its resolution and its recording speed are respectively set at (1080x720) and 30 *fps*. Its vertical and horizontal FOV are respectively equal to $FOV_v = 58.4^\circ$ and $FOV_u = 80^\circ$. Whereas, the IMU is considered as fixed on the camera and its measurements sampled at 30 *Hz*. Both sensors, the camera and the IMU, are assumed to be synchronized. Note that, plenty of conventional cameras and IMU can satisfy these specifications even low cost devices. The ROI is chosen large enough to capture the left, center and right lanes with $Y_{max} = -Y_{min} = 12$ m. As discussed in [7], $X_{max} = 30$ m and $X_{min} = 5$ m allow the rider to react in case of danger and to avoid blind spot consideration. Note that all the results below are given at X_0 which is the projection of the camera center on the ground.

In the present scenarios below, we assume the road to be planar (no elevation) and the curvature radius is constant at 232 m. In addition, the road is in good condition with a constant friction coefficient of 0.8. The motorcycle is moving at 100 *km/h* in a single 5 m wide traffic lane demarcated by a right and left solid lanes. For the simulations below, the right lane is considered as the reference. Indeed, in most cases, it is closer to the P2WV for right-hand drive and it is a solid lane. Nevertheless, it is utterly possible to consider other lane as a reference even if it is a dashed lane. Nevertheless, the estimation performances could be affected.

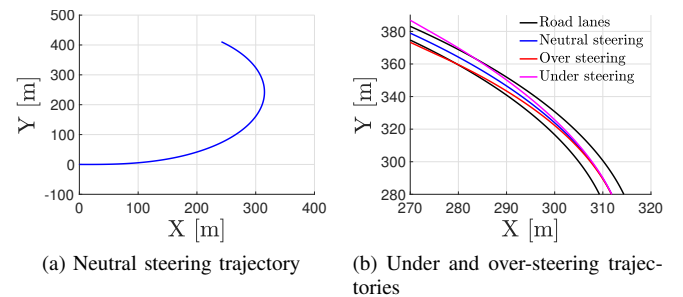


Fig. 3: Vehicle and road trajectories vs steering behavior

Figure 3 depicts the vehicle trajectories along the constant turns. We can clearly notice the over, neutral and under-steering behaviors, respectively in red, blue and magenta. Note that these colors are reused below. For the neutral case, the P2WV and road trajectories are equal. Nevertheless, for an under-steering motorcycle, it means the rider does not apply enough torque on the handlebar and the P2WV consequently tends to expand the curve. On the contrary, an over-steering behavior means the applied rider torque is too important regarding the road trajectory and the vehicle tends to cut the curve. Figure 4 highlights some of the P2WV dynamics states and the estimated kinematic ratio. Figure 4.a introduces the rider's torque, used to control the vehicle, and the induced steering angle. We can observe the torques used

to virtually generate the over and under-steering scenarios.

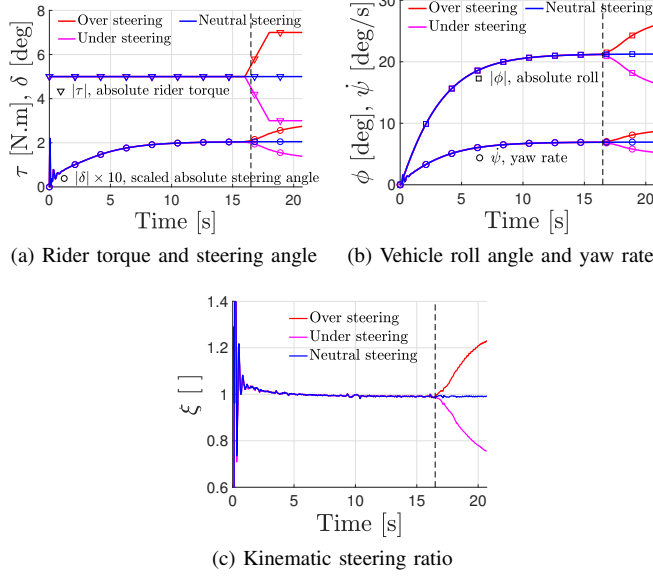


Fig. 4: Kinematic steering ratio vs vehicle dynamics

Note that, the nominal rider torque for the neutral trajectory is set at -5 N.m leading to a 0.2° steering angle. Note that, the initial conditions are defined such that the P2WV is entering in the curve with a null roll and steering angles. Figure 4.b introduces the vehicle roll angle and its yaw rate during the steady turn for the different steering behaviors. It shows that the over and under steering behaviors directly impact the roll angle. That is why, the vision algorithm must take into account the roll angle variations. In addition, the variation of the yaw rate turns out to be an interesting indicator to characterize the steering behavior. This topic is discussed below. Finally, Figure 4.c presents the steering ratio ξ computed since the kinematic approach given in (6) with (7) and (8). It clearly endorses the observations made in the previous section in remark 1. The dashed vertical line indicates the reference time when the steering ratio is significantly affected by over and under-steering. It has the same meaning in all figures below.

Figure 5 shows the estimations, in red, and the simulated data, in blue. They come from the clothoid model given in (4) with regard to the right lane. These last were estimated using the vision algorithm introduced in the previous section. We can notice that the (1080x720) image resolution allows to get great estimation results. Figures 5.a depicts the road trajectory. Whereas Figures 5.c-5.d and 5.e-5.f introduce the P2WV relative position to the right road marker, respectively for an under and over-steering scenario. As expected, an under-steered motorcycle gets closer and closer to the right lane until it crosses the lane. For an over-steering vehicle, it gets further and further from the right lane. Because the road sides are often filthy with sand, etc. These dangerous behaviors can lead to a vehicle loss of control and, in the worst case, to an accident. In this context, we propose a new vision-based approach to detect these kind of dangerous

steering behaviors.

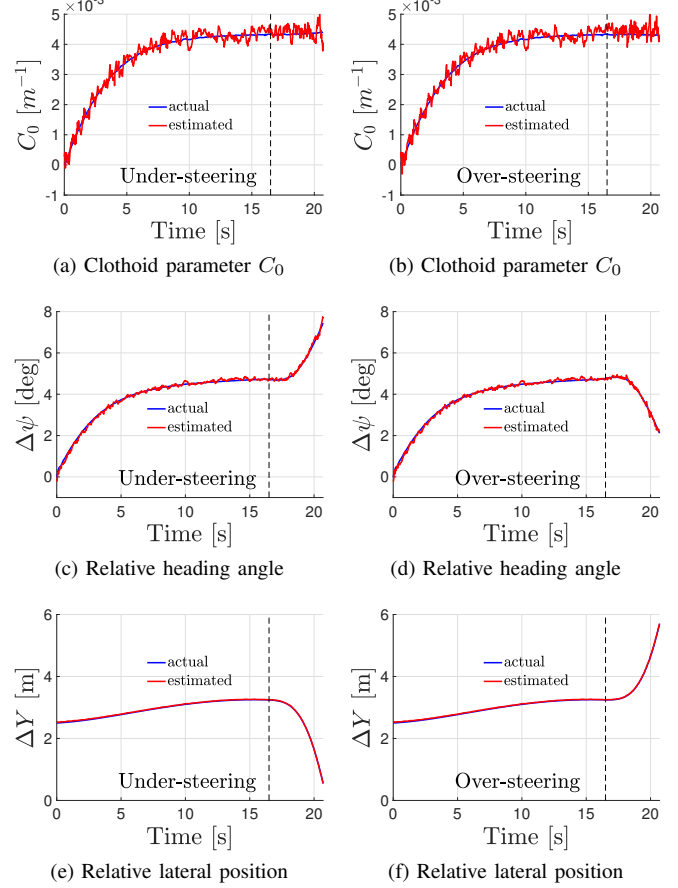


Fig. 5: Estimated parameters with the vision

A. Under-steering & Over-steering scenario

This subsection aims to introduce the under-steering and over-steering simulation results during a steady turn.

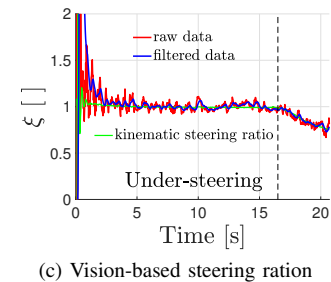
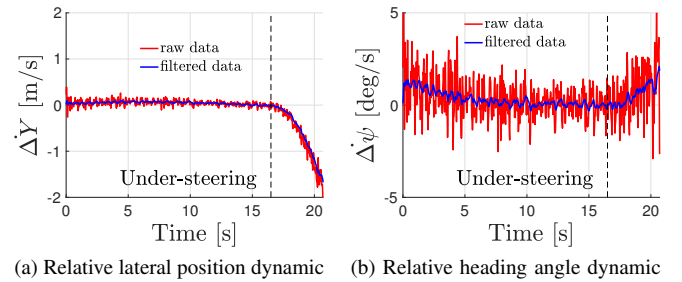


Fig. 6: Under-steering scenario vs vision-based indicators

Figure 6 depicts the pertinent indicators an under-steering case, whereas in Figure 7, the over-steering situation is addressed.

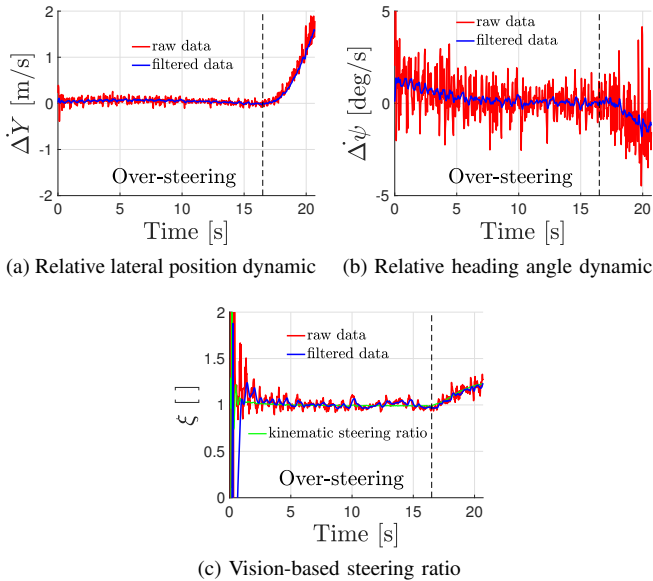


Fig. 7: Over-steering scenario vs vision-based indicators

B. Results discussion

Figures 6 and 7 highlight pertinent indicators for steering behavior characterization. As for the kinematic approach, we use the steering ratio computed thanks to vision. In addition, we propose to include two complementary indicators such that the time derivatives of the relative heading angle $\Delta\psi$ and the lateral position ΔY .

Note that these three dynamic states need to be filtered because of the estimation uncertainties. Even if the estimations introduced in Figures 5.c-5.f are barely affected by noise, it is amplified after the time derivation. To that end, we used a simple first order Butterworth filter.

Finally, the vision-based steering ratio presented in Figures 6.c and 7.c is very close to the one obtained with the kinematic approach. Then, the time derivative of the relative lateral position (Figures 6.a and 7.a) turns out to be a very interesting indicator. Indeed, this last is supposed to be near zero for neutral steering whereas, it suddenly changes for over or under-steering situations. Moreover, the ratio between the noise and the signal's amplitude is quite small. That makes $\Delta\dot{Y}$ a consistent indicator for steering characterization.

Furthermore, the time derivative of the relative heading angle $\Delta\dot{\psi}$ can be used as a background indicator to endorse the results. As Figures 6.c and 7.c depict, this variable is affected by noise. Nevertheless, even with significant noise, it allows to detect over or under-steering behavior as soon as it differs from zero.

V. CONCLUSION

The present paper deals with the assessment of motorcycle steering behavior in order to prevent dangerous situations

in turns. Indeed, the proposed approach is proficient in identifying under, neutral or over-steering behavior with two basic sensors: a conventional camera and an IMU. Based on the well-known clothoid model and the inverse perspective mapping technique, the both vehicle trajectory radius and road radius are recovered entirely without the need of some steady-state constraints or dynamics. In addition, no vehicle parameter and no steering encoder are required. These both radius are used to estimate the steering ratio ξ .

As well, we propose a new performance index for qualifying the steering behavior. This last is the dynamic of the relative lateral position $\Delta\dot{Y}$ between the motorcycle and the road. This index, emphasize much more the steering behavior because of an important signal to noise ratio comparing to ξ . We also proposed a second background indicator $\Delta\dot{\psi}$ which corresponds to the dynamics of the relative yaw angle.

Finally, simulations are carried out using a nonlinear multibody simulator called BikeSim. The results highlight the great capabilities of the proposed approach of characterizing the steering behavior in order to detect over and under-steering situations (links to videos <https://youtu.be/2UDpoS4QuVk> and <https://youtu.be/FgzHeQOEEdCo>).

In the near future, we would like to address the case of the non-steady turn and the validation on experimental data.

ACKNOWLEDGMENTS

This work is supported by National Agency of Research under the framework VIROLO++.

REFERENCES

- [1] ONSIR, "Accidentalit  routi re 2017-estimations au 25 janvier 2018," Observatoire national Interminist riel de la s curit  routi re (ONSIR), Tech. Rep., 2017.
- [2] B. Simpkin, F. Lai, K. Chorlton, and M. Fowkes, "Intelligent speed adaptation: Results of motorcycle trial," Ph.D. dissertation, University of Leeds, 2007.
- [3] F. Biral, M. Da Lio, R. Lot, and R. Sartori, "An intelligent curve warning system for powered two wheel vehicles," *European Transport Research Review*, 2010.
- [4] ACEM, "Motorcycle accidents in depth study (MAIDS)," ACEM (European Association of Motorcycle Manufacturers), Tech. Rep., 2009.
- [5] A. Pausie and L. Guillot, "Advanced telematics for enhancing the safety and comfort of motorcycle riders - benchmarking database," INRETS / LESCOT, Tech. Rep., 2008.
- [6] V. Cossalter, R. Lot, and M. Peretto, "Steady turning of motorcycles," *Proceedings of the Institution of Mechanical Engineers, Part D: Journal of Automobile Engineering*, vol. 221, no. 11, pp. 1343–1356, 2007.
- [7] P. M. Damon, H. Hadj-Abdelkader, H. Arioui, and K. Youcef-Toumi, "Image-based lateral position, steering behavior estimation, and road curvature prediction for motorcycles," *Robotics and Automation Letters*, vol. 3, no. 3, pp. 2694–2701, July 2018.
- [8] G. Casal, D. Santamarina, and M. E. Vzquez-Mndez, "Optimization of horizontal alignment geometry in road design and reconstruction," *Transportation Research Part C: Emerging Technologies*, 2017.
- [9] A. Z. E. D. Dickmanns, "A curvature-based scheme for improving road vehicle guidance by computer vision," *Proc.SPIE*, 1987.
- [10] T. B. Andres Hernandez-Gutierrez, Juan I. Nieto and E. M. Nebot, "Probabilistic road geometry estimation using a millimetre-wave radar," *Intelligent Robots and Systems (IROS)*, 2011.
- [11] V. Cossalter, *Motorcycle dynamics*. Lulu, 2006.
- [12] F. Busnelli, G. Panzani, M. Corno, and S. M. Savaresi, "Two-wheeled vehicles black-box sideslip angle estimation," *Conference on Decision and Control*, pp. 351–356, Dec 2017.